Supplement of Atmos. Chem. Phys., 25, 8163–8183, 2025
https://doi.org/10.5194/acp-25-8163-2025-supplement

Atmospheric Chemistry and Physics Open Access

Supplement of

Uncertainties in the effects of organic aerosol coatings on polycyclic aromatic hydrocarbon concentrations and their estimated health effects

Sijia Lou et al.

Correspondence to: Sijia Lou (lousijia@nju.edu.com) and Manish Shrivastava (manishkumar.shrivastava@pnnl.gov)

Text S1. Impact of OA coatings on BaP oxidation approaches

The oxidation lifetimes of particle-bound BaP, driven by ozone, vary from minutes to several hours. This variation depends on factors such as relative humidity (RH), substrate type, and ozone concentrations. In a previous global model simulation, applying the oxidation kinetics for BaP adsorbed onto soot aerosol particles, as reported by Pöschl et al. (2001), resulted in significant under-prediction of BaP concentrations compared to measurements taken at ground sites. In contrast, Zhou et al. (2012; 2013) measured slower oxidation kinetics for BaP adsorbed on ammonium sulphate particles coated with organics, making their findings more conservative. Furthermore, the oxidation of BaP is influenced by relative humidity (RH), occurring more rapidly under higher RH compared to dry conditions. These findings have significantly advanced PAH simulations, especially regarding lifetime estimates [Sehili and Lammel, 2007; Friedman and Selin, 2012; Shen et al., 2014; Shrivastava et al., 2017; Mu et al., 2018]. However, uncertainties remain in modeling the oxidation of particle-bound BaP, as it is sensitive to oxidant concentrations (mainly ozone) and the effectiveness of organic aerosol coatings, which are further influenced by temperature and RH. The main objective of this study is to identify the most accurate chemical schemes for simulating global BaP concentrations, evaluate the strengths and limitations of current PAH modeling approaches, and provide insights for future simulations improvements. To this end, we focus on comparing three OA coating schemes, with their first-order reaction rate coefficients k(s^{-1}) summarized in Table S1.

(1) NOA approach:

The heterogeneous oxidation of particle-bound BaP follows the Langmuir-Hinselwood mechanism. The reaction rate of BaP with O_3 proceeds at a rate k (s^{-1}) is given by Zhou et al. (2013) as:

$$k = \frac{k_{max} K_{O_3} [O_3]}{1 + K_{O_3} [O_3]}$$

where k_{max} is the maximum first-order rate coefficient for BaP loss, K_{O3} is the ozone gas-to-surface partition coefficient, and $[O_3]$ is the gas-phase ozone concentration (molec/cm^3). In this study, particle-bound BaP reacts rapidly with oxidants like ozone and OH radicals, and the oxidation kinetics measured by Zhou et al. (2012; 2013) for thin SOA coatings are applied consistently, irrespective of coating thickness or temperature and relative humidity variations.

(2) Shielded approach:

Based on our previous work (Shrivastava et al., 2017), the SOA Shielded approach is used to account for the protection of BaP by viscous SOA coatings. When BaP is coated by organic aerosols, the kinetics of its heterogeneous oxidation with ozone slow down significantly. This is because thick OA coatings hinder the mass transfer of BaP from the particle interior to the surface and BaP reacts at the particle surface with ozone. The effectiveness of this shielding depends on the thickness and viscosity of the SOA, which are influenced by temperature and relative humidity [Zhou et al., 2012; 2013]. In this approach, when SOA coatings are less than 20 nm, they are assumed to be ineffective in shielding particle-bound BaP. As a result, the heterogeneous oxidation kinetics remain unchanged, similar to the NOA approach (for thin SOA in Table R1). For thicker SOA coatings (> 20 nm), the heterogeneous oxidation of particle-bound BaP is essentially inhibited under dry or cool conditions (RH < 50% or temperature < 296 K). The oxidation kinetics of BaP with thick SOA coatings under varying humidity and temperature are measured by Zhou et al. (2012; 2013).

(3) ROI-T approach:

In accordance with Mu et al. (2018), the ROI-T approach is employed, which considers the temperature and humidity dependence of the phase state, diffusivity, and reactivity of particulate-phase BaP. The first-order reaction rate coefficients for BaP ozonolysis are highly sensitive to both temperature and RH at temperatures below room temperature (296 K), but they become primarily temperature-sensitive above this threshold [Mu et al., 2018]. Under cool and dry conditions, the first-order reaction rate coefficients are three orders of magnitude lower than those under warmer conditions (Table S1). Importantly, the ROI-T approach results in a much slower oxidation of particle-bound BaP compared to the NOA approach under cool, dry conditions but predicts a faster reaction rate under warmer conditions (e.g., 303K).

Text S2. BaP gas-particle partitioning

In our previous work, we explored the use of single-parameter linear free energy relationships (sp-LFER) to model the dual absorption-adsorption behavior in OA and black carbon (BC), an approach derived from Junge-Pankow's framework (Dachs and Eisenreich 2000; Lohmann and Lammel, 2004). The recently-developed pp-LFER approach, however, distinguishes itself by treating OA as consisting of two distinct phases: a liquid phase (comprising both water-soluble and organic-soluble components) and a semi-solid/solid organic polymer phase. In comparison, pp-LFER model predicts more than 90% of particle-bound BaP is absorbed by OA, while previous regional and global models suggest that most PAH is bound to BC (Friedman and Selin, 2012; Shen et al., 2014). This discrepancy is largely due to significant differences in partitioning coefficients used for BC in these models. Our previous work demonstrated that the *KBC-air* value derived from Lohmann and Lammel (2004) is two orders of magnitude higher than the pp-LFER-derived value at 298 K. This suggests that previous models may have overestimated the contribution of BC to particle-bound PAHs. Furthermore, using pp-LFER results in a moderate (~5-fold) increase at 298 K in the effective partitioning coefficient of BaP to OA compared to approaches such as Odabasi et al. (2006), which used n-octanol as a surrogate for OA. However, n-octanol is not an ideal surrogate for atmospheric OA due to its low water solubility and low polarity, making the pp-LFER approach, with its two-phase OA model, a more accurate representation of atmospheric SOA (Shahpoury et al., 2016).

Therefore, the choice of the pp-LFER approach over the Junge-Pankow model is driven by its more realistic representation of the complex partitioning behavior in the atmosphere, particularly the dual-phase nature of organic aerosol. For a global model, a unified approach is necessary to account for both remote and urban areas. While the Junge-Pankow model is effective for remote regions, the pp-LFER model offers a more accurate representation of urban and anthropogenically impacted areas, where both adsorption and absorption processes play significant roles. Further details can be found in our previous study Shrivastava et al., (2017).

Table S1. Comparison of first-order reaction rate coefficients (k, s^{-1}) across the three approaches, calculated at 50 ppb O_3. Note: The thickness of SOA coatings in the Shielded scheme must always be considered when interpreting the results.

	NOA	Shielded		ROI-T
Temperature		Thin SOA	Thick SOA	
	RH=70%			
303K	2.6×10^{-4}	2.6×10^{-4}	2.9×10^{-4}	5.8×10^{-4}
288K	2.7×10^{-4}	2.7×10^{-4}	0	1.6×10^{-4}
273K	2.9×10^{-4}	2.9×10^{-4}	0	4.0×10^{-5}
263K	3.0×10^{-4}	3.0×10^{-4}	0	1.6×10^{-5}
253K	3.1×10^{-4}	3.1×10^{-4}	0	5.6×10^{-6}
	RH=50%			
303K	2.6×10^{-4}	2.6×10^{-4}	0	5.7×10^{-4}
288K	2.7×10^{-4}	2.7×10^{-4}	0	1.5×10^{-4}
273K	2.9×10^{-4}	2.9×10^{-4}	0	2.2×10^{-5}
263K	3.0×10^{-4}	3.0×10^{-4}	0	2.0×10^{-6}
253K	3.1×10^{-4}	3.1×10^{-4}	0	1.8×10^{-7}
	RH=30%			
303K	2.6×10^{-4}	2.6×10^{-4}	0	5.3×10^{-4}
288K	2.7×10^{-4}	2.7×10^{-4}	0	1.0×10^{-4}
273K	2.9×10^{-4}	2.9×10^{-4}	0	4.3×10^{-6}
263K	3.0×10^{-4}	3.0×10^{-4}	0	4.9×10^{-7}
253K	3.1×10^{-4}	3.1×10^{-4}	0	1.5×10^{-7}

Table S2: 66 background sites information [*IADN*; *Hung et al.*, 2010; *Tørseth et al.*, 2012; *Shen et al.*, 2014; *Boruvkova*, 2015]

region	lat	lon	Location name	Obs. period
North America	47.5	–88.1	Eagle Harbor, MI	2005–2010
	43.8	–77.2	Point Petre, ON	2005–2010
	44.8	–86.1	Sleeping bear dunes, MI	2005–2010
	42.7	–79.1	Sturgeon point, NY	2005–2010
	45.8	–82.9	Burnt Island, ON	2005–2010
	33.9	–85.0	Yorkville, GA	2002, May
	39.2	–76.2	Chesapeake Bay, America	1997, summer
				1997, winter
	44.0	–121.7	Mount Bachelor Observatory	2004–2006, spring
Europe	40.6	22.9	Greater Athens Area, Greece	2001, May–2002, June
	42.0	13.3	Central Italy park, Italy	2000–2001
	43.3	5.5	Marseille, France, Plan d'Aups, rural	2004, July
	50.9	5.4	Hasselt, Flanders, Belgium	2002, spring
				2002, winter
	58.8	17.4	Aspvreten, Sweden	2005–2011
	58.4	8.3	Birkenes, Norway	2008–2009
	59.5	25.9	Lahemaa, Estonia	2007–2009
	47.9	7.9	Schauinsland, Germany	2007–2010
	50.7	10.8	Schmucke, Germany	2007–2010
	49.6	15.1	Kosetice, Czech Republic	2005–2011
	54.4	12.7	Zingst, Germany	2006–2009
	57.4	11.9	Rao, Sweden	2005–2011
	54.9	8.3	Westerland, Germany	2007–2010
	43.4	–4.9	Niembro	2004–2006, winter
	54.3	–0.8	High Muffles	2004–2007
	68.0	24.2	Pallas	2005–2011
	50.2	15	Europe group 1	2007–2011
	48.3	17.5	Europe group 2	2007–2011
	50.2	17.5	Europe group 3	2007–2011
	45.8	16.0	Zagreb, IMI	2007–2011
	47.0	19.6	K-puszta	2009–2011
	56.2	21.2	Rucava, EMEP	2009–2011
	46.5	28.3	Leova	2007–2011
	52.3	4.5	De Zilk	2009–2011
	54.1	22.0	Diabla Gora	2009–2011
	54.5	56.0	ERPC	2009–2011
	46.5	30.3	Petrodolinskoe	2009–2011
	42.6	23.1	Europe group 4	2007, Apr.– Aug.
	42.0	24.8	Plovdiv, UBMS Dolni Voden	2007, Apr.– Aug.
	50.2	12.5	Europe group 5	2009, Feb.–June
	50.2	17.5	Europe group 6	2010, Feb.–June
	50.2	15.0	Europe group 7	2008–2011, Sep.-Mar.
	50.2	20.0	Europe group 8	2007, Apr.– Aug.
	50.1	12.4	Cheb	2008, Sep.–Dec.
	50.5	13.4	Chomutov	2008–2011, Sep-Mar
	49.1	13.6	Churanov, Sumava	2007–2011, June-Dec
	48.9	14.3	Klet, Sumava	2007–2009, July-Dec
	50.5	13.6	Most	2008–2011, Aug–Feb
	56.0	21.9	Plateliai	2010, June–2011, Jan
	55.4	26.1	Rugsteliskes	2008–2010, Nov–Feb

	55.1	36.6	Obninsk	2009–2010, Sep–Dec
	55.4	21.1	Preila	2008–2010, Oct–Mar
	49.0	22.3	Starina	2009–2011, July-Mar
	50.6	30.5	Oseshchyna	2008, May–2008, Sep
	45.3	30.2	Zmiinyi Island	2009–2011, July–Dec
	46.5	29.5	Stefan Voda	2007, Apr.– Aug.
	42.4	19.3	Podgorica	2007, Apr.– Aug.
	46.5	15.7	Maribor OZADSE	2007, Apr.– Aug.
Africa	–4.3	15.2	Brazzaville, Congo	2008–2011
	6.7	–0.8	Abetefi, Ghana	2010–2011
	–20.2	57.5	Reduit	2008–2011
	8.9	7.1	Sheda	2008–2011
	15.6	32.5	Khartoum, Sudan	2008–2011
Asia	37.4	136.9	Wajima, Japan	2005, May–Sep.
				2004, Oct.–2005, Apr.
	37.5	121.4	Yantai, China	annual
	40.7	45.0	Asia group 1	2008, June–Nov.
	47.1	51.9	Atyrau	2008, Apr.–Aug.
	49.8	73.1	Karaganda	2008, Apr.–Aug.

Table S3: 208 non-background sites information [*IADN*; *Hung et al.*, 2010; *Tørseth et al.*, 2012; *Shen et al.*, 2014; *Boruvkova*, 2015]

region	lat	lon	Location name	Obs. period
North America	34.0	-118.1	Long Beach Freeway, Los Angeles Basin	2004, May-June 2005, Jan.
	34.1	-118.2	the California State Highway, Los Angeles Basin	2004, May-June 2005, Jan.
	34.1	-118.2	the California State Highway, Los Angeles Basin	2006, Feb.-June.
	29.8	-95.4	Houston	1991
	40.5	-74.4	New Brunswick, NJ	1997, Oct.–1998, Oct.
	42.4	-71.1	Boston	1991
	44.3	-79.9	Borden, Ontario, Canada	2001, Oct.–2002, Dec.
	41.7	-87.6	Chicago, USA	2004, Winter
	41.9	-87.6	Chicago, USA	1995, Summer
	41.9	-87.6	Chicago, America	2004, Summer
	34.2	-118.2	Los Angeles	2005, Winter
	34.1	-117.9	Los Angeles	2005, Winter
	34.1	-118.2	Los Angeles, USA	1976, Winter
	27.7	-82.7	Gulfport, FL	2002, May
	28.0	-82.2	Sydney, Fla	2002, May
	33.8	-84.4	Jefferson St, GA	2002, May
	30.4	-89.1	Gulfport, MS	2002, May
	43.8	-71.8	Thompson Farm, NH	2002, May
	41.9	-87.6	Chicago, America	1995, Summer
	34.1	-118.2	Los Angeles, USA	1976, Summer
	39.1	-76.6	Baltimore, America	1997, July
Europe	38.0	23.7	Athens, Greece	2003, Dec.–2004, Feb.
	60.2	25.0	Helsinki, Finland	2002, Jan.
	60.2	25.0	Helsinki, Finland	2002, Feb
	61.9	25.7	Kurkimäki, Finland	2006, winter
	61.9	25.7	Kurkimäki, in Central Finland	2006, Winter
	50.1	14.4	Prague 5—Smichov	2004, Jan.
	50.1	14.4	Prague, Czech Republic	2005, Nov.-Dec.
	43.8	11.1	Bagnoli	2005, Nov.-Dec.
	51.3	4.5	Point-source	2002
	51.2	4.5	Residential	2002
	52.5	-1.9	Birmingham, UK	1996, Winter
	51.0	-3.7	Borgerhout, Flanders, Belgium	2001, Nov.-Dec.
	51.0	-3.7	Mechelen, Flanders, Belgium	2002, Nov.-Dec.
	51.0	-3.7	Zelzate, Flanders, Belgium	2002, Winter
	51.0	-3.7	Petroleumkaai, Flanders, Belgium	2003, Winter
	43.2	131.9	Vladivostok, Russia	1999, Winter
	51.5	7.0	Essen, Germany	1981, Winter
	45.2	9.2	Pavia, Italy	1996, Feb.-June
	40.6	22.9	Greater Athens Area, Greece	2001, May–2002, June
	44.5	18.7	Tuzla	2004, May
	44.5	18.7	Tuzla，Herzegovina	2004, May
	43.8	18.3	Sarajevo	2004, May
	43.8	18.3	Sarajevo，Bosnia	2004, May
	51.0	-3.7	Borgerhout, Flanders, Belgium	2003, Apr.-May

	50.4	18.8	Repty S´ la¸ skie, Poland	1995, May
	45.5	10.2	Brcscia, Lombardy, Italy	1991, Mar.-May
	45.7	7.3	Aosta, Italy	1995, Mar.
	38.0	23.7	Koropi, Athens, Greece	2003, July-Dec.
	38.0	23.7	Spata, Athens, Greece	2003, July-Dec.
	38.0	23.7	Athens, Greece	2003, June-Nov.
	38.0	23.7	Athens, Greece	2004, May-July
	60.2	25.0	Helsinki, Finland	2001, Sep.-Oct.
	50.1	14.4	Prague, Czech Republic	2000, Summer
	43.8	11.1	Bagnoli	2000, Summer
	43.3	5.5	Marseille, France, Penne, sub-urban	2004, July
	43.3	5.4	Marseille, France, 5 avenues, urban	2004, July
	52.5	-1.9	Birmingham, UK	1996, Summer
	43.2	131.9	Vladivostok, Russia	1999, Summer
	51.5	7.0	Essen, Germany	1981, Summer
	51.2	3.8	Flanders, Belgium	2002, Sep.-Nov.
	50.1	14.4	Prague, Czech Republic	2004, Sep.
	51.2	4.4	Petroleumkaai, Flanders, Belgium	2001, Sep.
	51.0	4.5	Flanders, Belgium	2002, Sep.-Nov.
	40.6	22.9	MAR	2001, May–2002, June
	40.6	22.9	ARI	2001, May–2002, June
	40.6	22.9	ELE	2001, May–2002, June
	40.6	23.0	Thessaloniki, Greece	1996, Jan.–1997, Feb.
	50.1	14.4	Prague, Czech Republic	2000, Apr.–2001, Mar.
	57.2	14.6	Ro¨ rvik	1994–1999
	57.2	14.6	Pallas	1996–1999
	43.8	11.1	Bagnoli	2000, Dec.–2001, July
	44.5	11.3	Bologna, Italy	2003
	43.9	11.1	Prato (Italy)	2003, Mar.-Nov.
	51.5	-0.2	London	1991–1998
	51.5	-0.2	London	1992
	43.3	-1.9	Errenteria	1996, Feb.–1997, Dec.
	43.3	-1.9	Errenteria, Basque Country, Spain	1996, Jan.–1997, Dec.
	51.3	12.4	Leipzig, Germany.	1999–2002
	53.5	10.0	Wervikstraat,border between Belgium and France	2003
	41.4	2.2	Barcelona, Spain	2004–2005
	53.5	-2.2	Mancherster	1991–1998
Asia	43.1	141.4	Sapporo, Japan	1997, Winter
	43.1	141.4	Sapporo, Japan	1997, Winter
	35.7	139.7	Tokyo, Japan	1997, Winter
	35.7	139.7	Tokyo, Japan	1997, Winter
	36.6	136.6	Kanazawa, Japan	1999, Winter
	36.6	136.6	Kanazawa, Japan	1999, Winter
	37.6	127.0	Seoul, South Korea	2002, Winter
	37.6	127.0	Seoul, South Korea	2002, Winter
	39.9	116.4	Beijing, China	2005, Dec.–2006, Jan.
	22.3	114.1	Hung Hom (PU)	2000, Nov.–2001, Feb.
	23.1	113.4	Wushan, Guangzhou, China	2004, Jan.
	23.1	113.3	Guangzhou, China	2003, Winter
	23.1	113.3	Guangzhou, China	2004, Jan.
	11.0	106.6	Ho Chi Minh City，Vietnam	2005, Jan.–2006, Mar.
	39.8	28.9	Bursa, Turkey	2005, Jan.-Feb.

35.0	138.4	Shimizu	2001, Winter
33.9	130.8	Kitakyushu, Japan	1997, Winter
41.9	123.4	Shenyang, China	2001, Winter
3.2	101.7	Kuala Lumpur, Malaysia	1998, Sep.–1999, Jan.
26.8	80.9	Lucknow city, India	2005, Feb.
38.9	127.1	Dalian, China	2004
40.0	116.4	Beijing, China	2004
23.1	113.3	Guangzhou, China	2003
23.1	113.4	Wushan, Guangzhou, China	2004, Apr.
23.1	113.3	Guangzhou, China	2004, Apr.
22.8	108.3	Yulin, Guangxi, China	2004, Mar.–Apr.
22.8	108.3	Yulin, Guangxi, China	2004, Mar.
34.7	135.5	Osaka, Japan	2005, Apr.–2006, May
31.2	121.5	Shanghai, China	2004, Mar.-Apr.
43.1	141.4	Sapporo, Japan	1997, Summer
43.1	141.4	Sapporo, Japan	1997, Summer
35.7	139.7	Tokyo, Japan	1997, Summer
35.7	139.7	Tokyo, Japan	1997, Summer
36.6	136.6	Kanazawa, Japan	1999, Summer
36.6	136.6	Kanazawa, Japan	1999, Summer
39.1	117.3	Tianjin	2005, July-Aug.
39.1	117.3	Tianjin	2005, July-Aug.
39.1	117.3	Tianjin	2005, July-Aug.
22.3	114.1	Kwun Tong (KT)	2001, June-Aug.
22.3	114.2	Hung Hom (PU)	2001, June-Aug.
23.1	113.4	Wushan, Guangzhou, China	2003, Aug.
23.1	113.3	Guangzhou, China	2003, Summer
23.1	113.3	Guangzhou, China	2002, Summer
39.8	28.9	Bursa, Turkey	2004, July-Aug.
34.7	135.5	Osaka, Japan	2005, Apr.–2006, May
33.9	130.8	Kitakyushu, Japan	1997, Summer
41.9	123.4	Shenyang, China	2001, Summer
23.7	121.0	Taiwan,suburban	Annual
23.1	113.3	Guangzhou, China	2002, Sep.-Nov.
23.1	113.3	Guangzhou, China	2003, Nov.
23.1	113.4	Wushan, Guangzhou, China	2003, Nov.
35.2	138.7	Shizuoka, Japan	2001, Feb.–2002, Jan.
35.0	138.4	Shizuoka, Japan	2001, Feb.–2002, Jan.
38.9	121.5	Dalian, China	Annual
37.6	127.0	Seoul, Korea	1993, Mar.-Dec.
37.6	127.0	Seoul, Korea	1998, Oct.–1999. Dec
32.1	118.8	Nanjing, China	2001–2002
32.1	118.8	Nanjing urban, China	2001–2002
24.5	118.1	Xiamen	2005
24.5	118.1	Xiamen	2005
24.9	118.0	Xiamen	2005
37.6	116.7	Dezhou, China	Annual
37.4	116.3	Dezhou, China	Annual
23.1	113.3	Gunagzhou, China	2001, Apr.–2002, Mar.
40.0	116.3	Beijing, China	Annual
22.4	114.1	Hong Kong	Annual
22.3	114.1	Kwun Tong (KT)	2000, Nov.–2001, Mar.
37.9	112.1	Taiyuan, China	Annual

	37.9	112.5	Taiyuan, China	Annual
	10.8	106.7	VNU, Vietnam National University	2005, Jan.–2006, Mar.
	10.8	106.7	DOSTE	2005, Jan.–2006, Mar.
	10.8	106.7	ITTE	2005, Jan.–2006, Mar.
	38.9	106.1	Yinchuan, China	Annual
	38.9	106.1	Yinchuan, China	Annual
	38.1	102.7	Wuyi, China	Annual
	37.9	102.6	Wuyi, China	Annual
	23.5	88.4	Kolkata (Calcutta), India	2003, Nov.–2004, Nov.
	23.5	88.4	Kolkata (Calcutta), India	2003, Nov.–2004, Nov.
	28.6	77.2	New Delhi, India	2003
	28.6	77.2	New Delhi, India	2002
	28.6	77.2	New Delhi, India	2001, Apr.–2002, Mar.
	31.5	74.3	Lahore, Pakistan	1992, Sep.–1993, Oct.
	31.5	74.3	Lahore, Pakistan	1992, Sep.–1993, Oct.
	31.5	74.3	Lahore, Pakistan	1992, Sep.–1993, Oct.
	40.2	29.0	Merinos, Turkey	2004, Aug.–2005, Apr.
	40.2	29.1	Merinos, Turkey	2004, Aug.–2005, May
	39.8	28.9	Bursa, Turkey	2004, Aug.–2005, Apr.
	34.4	132.8	Higashi Hiroshima, Japan	2006, Jan.–2007, Jan.
	32.8	129.9	Nagasaki city, Japan	1997, July–1998, June
	35.2	128.6	Changwon-Masan, Korea	2004, Oct.-Nov.
	35.9	127.8	Korea	2002
	37.4	121.5	Yantai, China	Annual
	23.7	120.6	Tunghai university, Taiwan	2001, Aug.–2002, Apr.
	-6.3	106.9	Jakarta, Indonesia	1992, Dec.–1993, Dec.
	1.3	103.8	Singapore	1994
	3.0	101.7	university of Malaya	2001, Mar.-Dec.
	15.9	101.0	Thailand	2000
	13.8	100.5	Bangkok, Thailand	1993, Apr.-Oct. 1994, Feb.-Apr.
	19.0	72.9	The creek adjoining Mumbai harbour, India	2000, June–2001, May
	40.4	116.9	Miyun	2004, Mar.-May
	36.7	3.1	Oued Smar, Algeria	2002, Aug.–Sep.,
Africa	36.7	3.1	Oued Smar, Algeria	2002, Nov.–2003, Feb.
	-37.8	145.0	Melbourne, Australia	1993
Oceanic	-27.7	153.0	Brisbane, Australia	2002, Winter
	-27.7	153.0	Brisbane, Australia	1998, Winter
	-27.7	153.0	Brisbane, Australia	1998, Summer
	-27.5	153.0	Brisbane, Australia	2004, Summer
	-34.9	-58.0	La Plata, Argentina	2000–2002
South America	-34.9	-58.0	La Plata, Argentina	1999–2002
	-34.9	-58.0	La Plata, Argentina	2000–2002
	-34.9	-58.0	La Plata, Argentina	2000–2002
	-30.0	-51.2	Metropolitan Area of Porto Alegre (MAPA), Brazil	2002–2005
	-31.7	-54.1	Candiota region, Brazil	2001, Feb.-Oct.
	-30.0	-51.2	Metropolitan Area of Porto Alegre, Rio Grande do Sul, Brazil	2001, Oct.–2002, Dec.
	-30.0	-51.6	Charqueadas	2001, Oct.–2002, Dec., Winter
	-30.0	-51.2	CEASA	2001, Oct.–2002, Dec., Winter

	-30.0	-51.2	Porto Alegre, Brazil	2002, Mar.-May
	-22.8	-43.2	Rio de Janeiro, Brazil	1998, Nov.
	-23.7	-46.6	Sao Paulo City, Brazil	2000, Aug.-Dec.
	-23.6	-46.6	Sao Paulo City, Brazil	2002, May-July
	-20.5	-54.7	Indubrasil	2003, July-Dec.
	-20.4	-54.6	Campo Grande City, Brazil	1998, July-Nov.
	-20.4	-54.6	Campo Grande, Brazil	2003, July-Dec.
	-20.4	-54.6	Campo Grande, Brazil	2003, July-Dec.

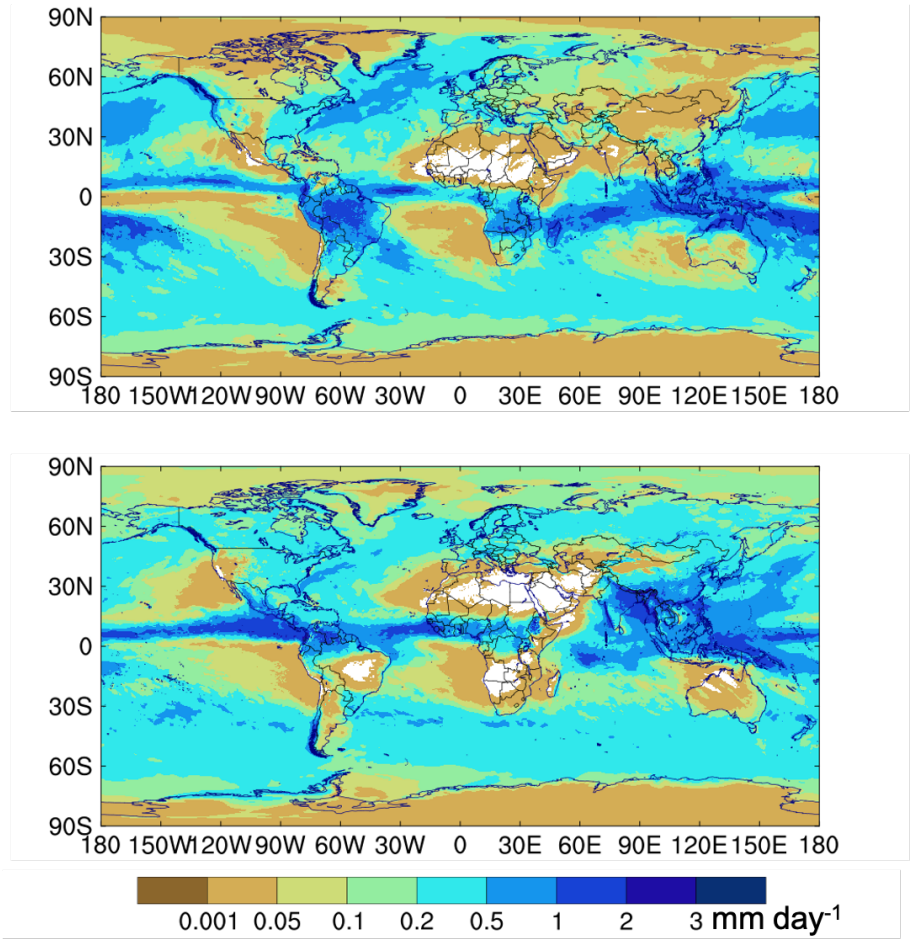

Figure S1. The spatial distribution of surface-layer average precipitation (unit: mm day^{-1}) in DJF (December-January-February) and JJA (June-July-August), respectively.

References

Boruvkova, J.: GENASIS-Global Environmental Assessment and Information System, version 2.0., Masaryk University, www.genasis.cz., 2015.

Dachs, J., and Eisenreich, S. J.: Adsorption onto aerosol soot carbon dominates gas-particle partitioning of polycyclic aromatic hydrocarbons, Environ. Sci. Technol., 34(17), 3690-3697, https://doi.org/10.1021/es991201+, 2000.

Friedman, C. L. and Selin, N. E.: Long-range atmospheric transport of polycyclic aromatic hydrocarbons: A global 3-D model analysis including evaluation of Arctic sources, Environ. Sci. Technol., 46(17), 9501-9510, https://doi.org/10.1021/es301904d, 2012.

Hung, H., Kallenborn, R., Breivik, K., Su, Y., Brorström-Lundén, Olafsdottir, K., Thorlacius, J. M., Leppänen, S., Bossi, R., Skov, H., Manø, S., Patton, G. W., Stern, G., Sverko, E., Fellin, P.: Atmospheric monitoring of organic pollutants in the Arctic under the Arctic Monitoring and Assessment Programme (AMAP): 1993-2006, Sci. Total Environ., 408(15), 2854-2873, doi:10.1016/j.scitotenv.2009.10.004.

IADN: The Integrated Atmospheric Deposition Network (IADN), https://www.ec.gc.ca/rs-mn/default.asp?lang=En&n=BFE9D3A3-1.

Lohmann, R., and Lammel, G.: Adsorptive and absorptive contributions to the gas-particle partitioning of polycyclic aromatic hydrocarbons: state of knowledge and recommended parametrization for modeling, Environ. Sci. Technol., 38(14), 3793-3803, https://doi.org/10.1021/es035337q, 2004.

Mu, Q., Shiraiwa, M., Octaviani, M., Ma, N., Ding, A., Su, H., Lammel, G., Poschl, U., and Cheng, Y.: Temperature effect on phase state and reactivity controls atmospheric multiphase chemistry and transport of PAHs, Sci. Adv., 4(3), doi:10.1126/sciadv.aap7314, 2018.

Odabasi, M., Cetin, E., Sofuoglu, A.: Determination of octanol-air partition coefficients and supercooled liquid vapor pressures of PAHs as a function of temperature: Application to gas-particle partitioning in an urban atmosphere, Atmos. Environ., 40(34), 6615-6625, https://doi.org/10.1016/j.atmosenv.2006.05.051, 2006.

Shrivastava, M., Lou, S., Zelenyuk, A., Easter, R. C., Corley, R. A., Thrall, B. D., Rasch, P. J., Fast, J. D., Massey Simonich, S. L., Shen, H., and Tao, S.: Global long-range transport and lung cancer risk from polycyclic aromatic hydrocarbons shielded by coatings of organic aerosol, Proc. Natl. Acad. Sci. U.S.A., 114(6), 1246-1251, https://doi.org/10.1073/pnas.1618475114, 2017.

Pöschl, U., Letzel, T., Schauer, C., and Niessner, R.: Interaction of ozone and water vapor with spark discharge soot aerosol particles coated with benzo [a] pyrene: O3 and H2O adsorption, benzo [a] pyrene degradation, and atmospheric implications, J. Phys. Chem. A, 105(16), 4029-4041, https://doi.org/10.1021/jp004137n, 2001.

Sehili, A. M., and Lammel, G.: Global fate and distribution of polycyclic aromatic hydrocarbons emitted from Europe and Russia, Atmos. Environ., 41(37), 8301-8315, https://doi.org/10.1016/j.atmosenv.2007.06.050, 2007.

Shahpoury, P., Lammel, G., Albinet, A., Sofuoglu, A., Dumanoglu, Y., Sofuoglu, S. C., Wagner, Z., and Zdimal, V.: Evaluation of a Conceptual Model for Gas-Particle Partitioning of Polycyclic Aromatic Hydrocarbons Using Polyparameter Linear Free Energy Relationships, Environ. Sci. Technol., 50(22), 12312-12319, https://doi.org/10.1021/acs.est.6b02158, 2016.

Shen, H., Tao, S., Liu, J., Huang, Y., Chen, H., Li, W., Zhang, Y., Chen, Y., Su, S., Lin, N., Xu, Y., Li, B., Wang, X., and Liu, W.: Global lung cancer risk from PAH exposure highly depends on emission sources and individual susceptibility, Sci. Rep., 4, 6561, https://doi.org/10.1038/srep06561, 2014.

Tørseth, K., Aas, W., Breivik, K., Fjæraa, A. M., Fiebig, M., Hjellbrekke, A.-G., Lund Myhre, C., Solberg, S., and Yttri, K. E.: Introduction to the European Monitoring and Evaluation Programme (EMEP) and observed atmospheric composition change during 1972–2009, Atmos. Chem.
Phys., 12(12), 5447-5481, doi:10.5194/acp-12-5447-2012, 2012.

Zhou, S., Lee, A. K. Y., McWhinney, R. D., and Abbatt, J. P. D.: Burial Effects of Organic Coatings on the Heterogeneous Reactivity of Particle-Borne Benzo a pyrene (BaP) toward Ozone, J. Phys. Chem. A, 116(26), 7050-7056, https://doi.org/10.1021/jp3030705, 2012.

Zhou, S., Shiraiwa, M., McWhinney, R. D., Poschl, U., and Abbatt, J. P.: Kinetic limitations in gas-particle reactions arising from slow diffusion in secondary organic aerosol, Faraday Discuss, 165, 391-406, https://doi.org/10.1039/C3FD00030C, 2013.